Magnetic Resonance Imaging, Vol. 11, pp. 341-355, 1993
Printed in the USA.

0730-725X/93 $6.00 + .00

● *Original Contribution*

A CHEMICAL SHIFT SELECTIVE INVERSION RECOVERY SEQUENCE FOR FAT-SUPPRESSED MRI: THEORY AND EXPERIMENTAL VALIDATION

ELENI KALDOUDI,* STEVE C.R. WILLIAMS,† GARETH J. BARKER,‡ AND PAUL S. TOFTS‡
*University College London, †Queen Mary and Westfield College, and ‡Institute of Neurology, London, UK

Fat-suppression techniques are used extensively in routine proton nuclear magnetic resonance imaging to produce images free from chemical shift artifacts and dynamic range problems. A hybrid fat-suppression sequence is studied which combines the principle of short time inversion recovery with chemical shift selective imaging. The aim of this study is to provide a theoretical understanding of the role of the sequence parameters, as well as to compare this hybrid sequence with its most closely related conventional fat-suppression techniques, namely selective presaturation and short time inversion recovery (STIR) imaging. The hybrid technique is shown to be robust in normal use, and more tolerant than the conventional methods to mis-settings of parameters such as inversion time, as well as tip angle and frequency bandwidth of the fat selective pulse.

Keywords: **MRI, Fat suppression; Selective inversion recovery; Short time inversion recovery (STIR); Selective presaturation.**

INTRODUCTION

Differentiation between fat and water is an important issue in proton magnetic resonance imaging (MRI). Numerous techniques have been proposed that create separate fat and water images or suppress contribution from one or the other. These include chemical shift and coupled spin imaging as well as techniques based on relaxation time and other chemical or physical differences.[1] Certain studies have reported the use of a "fat-only" image to extract additional diagnostic information,[2,3] but in general fat-suppression techniques are mainly used in clinical MRI to produce "water-only" images free from both chemical shift artifacts and partial volume effects, and to reduce dynamic range problems. Imaging time, software and hardware limitations, and the multi-slice requirement in most routine clinical MRI examinations do, however, restrict the wide use of many of these proposed fat-suppression techniques. The two most commonly used methods are the short inversion time inversion recovery (STIR) sequence and the selective presaturation (FATSAT) sequence.

The STIR sequence[4] has found widespread use in clinical imaging of various organs and regions, such as the musculoskeletal system.[5] It is especially favoured not only for its suppression of the fat signal, but also because it provides high T_1 contrast. The method also has no special hardware or software requirements, works in a multi-slice mode, and can be implemented on most clinical systems irrespective of both the static magnetic field strength and homogeneity. One significant disadvantage of the STIR sequence, however, is that it produces images with relatively poor signal-to-noise ratio (S/N) due to less than total recovery of the longitudinal magnetization of water.[6] In the extreme case, water signal from any tissue with T_1 comparable to that of fat is substantially suppressed. Furthermore, fat suppression using STIR sequences is heavily dependent on the T_1 of fat, which has to be either measured or at least estimated prior to the experiment. If the T_1 of fat is not accurately known, or the fat tissue exhibits a multi-exponential T_1 relaxation, STIR may result in inadequate fat suppression.

Fat saturation chemical shift imaging sequences[7-9] produce fat suppressed images without S/N degradation, although they require a static magnetic field homogeneous enough to allow differentiation between the resonance frequencies of the fat and water protons over the whole imaging volume. The method can function

RECEIVED 8/17/92; ACCEPTED 11/10/92.
Address correspondence to E. Kaldoudi, NMR Imaging Facility, Department of Chemistry, Queen Mary and Westfield College, Mile End Road, London E1, UK.

in a multi-slice mode, where the initial fat selective pulse and the subsequent spoiling magnetic field gradient are performed before the selection of each individual slice. However, the time required for the application of the spoiling gradient may be long enough for the short T_1 fat magnetization to recover to a value that would give a detectable signal on application of the following conventional spin echo part of the sequence.

In this paper we study a new hybrid fat suppression imaging sequence, which combines the principle of the STIR technique with selective irradiation of the fat protons to produce multi-slice data sets with enhanced fat suppression and without the limitations of the original techniques. Compared to STIR, fat-suppression by the hybrid sequence is less strongly dependent on the T_1 of fat. Furthermore, the inversion time required by this hybrid sequence is generally shorter than in STIR, thus allowing the imaging of more slices within the same repetition time, as well as manipulation of the contrast for the water signal to be T_1 and/or T_2 weighted, depending on the repetition and echo times, respectively. When compared to FATSAT, the hybrid sequence is more able to tolerate mis-settings in the tip angle and the frequency bandwidth of the selective pulse, thus reducing the rather stringent static and radiofrequency (RF) field requirements of this conventional chemical shift imaging method. The hybrid sequence is evaluated both using phantoms and in vivo, and is compared to conventional STIR and FATSAT imaging. We will refer to this hybrid sequence as CSS-IR (chemical shift selective-inversion recovery) hereafter. The method can also be regarded as a specific case of the selective partial inversion recovery (SPIR) sequence,[10] which has recently been implemented in the clinical evaluation of breast disease.[11]

THEORY

The pulse sequence diagram for CSS-IR is shown in Fig. 1. The initial 180° pulse is chemical shift selective, inverting only the fat protons, whose resonance frequencies lie within a ~2 ppm range centered ~3.6 ppm upfield of the water resonance. This causes the methyl (−CH3) and methylene (>CH2) protons of fat in the whole sample to be inverted while leaving the water magnetization unperturbed. A slice selective 90° pulse is then applied at a time $TI_{CSS\text{-}IR}$ when the inverted magnetization passes through the null point and causes only "non-inverted" protons within that slice (mainly the −OH group of both fat and water) to be excited. The sequence can function in a multi-slice fashion; although the fat magnetization of the whole sample is inverted, after the time $TI_{CSS\text{-}IR}$ + TE this signal has relaxed to a positive value, thus enabling the immediate repetition of the sequence to select a further slice.

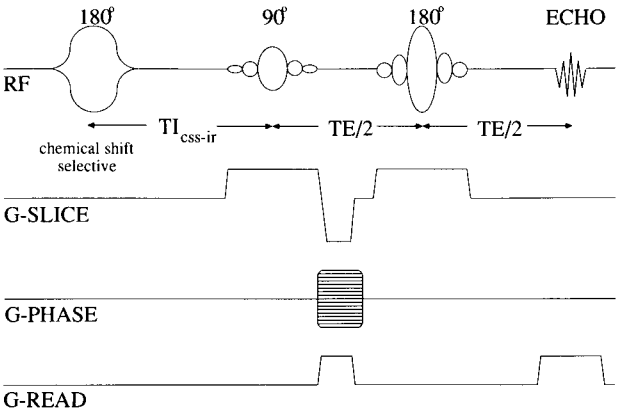

Fig. 1. Diagrammatic representation of the CSS-IR hybrid pulse sequence for fat suppression. The chemical shift selective 180° pulse inverts only the fat protons, and the inversion time, $TI_{CSS\text{-}IR}$, corresponds to the "null-point" for this magnetization. TE is the echo time.

For both STIR and CSS-IR, the inversion time TI, which corresponds to the time when the fat magnetization is zero, can be calculated considering the relaxation of the longitudinal magnetization M_z, as described by the Bloch equation:

$$\frac{dM_z}{dt} = -\frac{M_z - M_o}{T_1} \tag{1}$$

where M_o is the longitudinal thermal equilibrium magnetization. (In the following analysis steady-state-free-precession (SSFP) effects have been ignored, i.e., we assume $T_2 \ll$ TR.)

For the conventional STIR sequence this inversion time, TI_{STIR}, is given by:

$$TI_{STIR} = T_1 \ln 2 \tag{2}$$

where T_1 is assumed to be much shorter than the repetition time, that is, $T_1 \ll$ TR. Equation (2) is derived directly from the Bloch equation, noting that, due to the finite amount of T_1 relaxation which occurs during the time interval between the 90° read pulse and the next repetition of the sequence, the longitudinal magnetization M_z just before the inversion pulse is given by:

$$M_{z(STIR)} = M_o(1 - e^{-(TR - TI_{STIR})/T_1}) \; . \tag{3}$$

The situation, however, is different for the hybrid CSS-IR sequence. Here, as the inverting 180° pulse is applied in the absence of all gradients (in order to achieve chemical shift selection), its effect is not confined to a single slice. Therefore the fat protons over the whole

imaging volume experience a train of inverting pulses, with an effective repetition time:

$$TR_{eff} = \frac{TR}{N} \tag{4}$$

where N is the number of slices. (This is similar to the FATSAT sequence, where the fat protons experience a train of 90° pulses with the same effective repetition time, TR_{eff}.)

In the general case of a train of $\beta°$ pulses applied with a repetition time of TR_{eff}, the fat magnetization, M_n, just after the nth pulse can be calculated by integrating Eq. (1) with appropriate limits:

$$M_n(\beta°) = M_o \frac{\cos\beta(e^{-(TR_{eff}/T_1)} - 1) + \cos^n\beta\, e^{-n(TR_{eff}/T_1)}(\cos\beta - 1)}{\cos\beta\, e^{-(TR_{eff}/T_1)} - 1} \tag{5}$$

After many repetitions (i.e., as n tends to infinity), a steady state is reached and the fat magnetization is given by:

$$M_{ss}(\beta°) = M_o \frac{\cos\beta(e^{-(TR_{eff}/T_1)} - 1)}{\cos\beta\, e^{-(TR_{eff}/T_1)} - 1} \tag{6}$$

For the CSS-IR sequence, the longitudinal magnetization M_n and its steady state value M_{ss} can be directly derived from Eqs. (5) and (6) respectively, by setting the tip angle $\beta°$ equal to 180°:

$$M_n = M_o \frac{e^{-(TR_{eff}/T_1)} - 1 + 2(-1)^n e^{-n(TR_{eff}/T_1)}}{e^{-(TR_{eff}/T_1)} + 1} \tag{7}$$

and

$$M_{ss} = M_o \frac{e^{-(TR_{eff}/T_1)} - 1}{e^{-(TR_{eff}/T_1)} + 1} \; . \tag{8}$$

Figure 2A shows the fat magnetization M_n just after each inverting pulse as it approaches its steady state value. We assume a T_1 of 200 msec for fat and an effective repetition time of 250 msec (corresponding, for example, to a 10-slice data set with TR = 2500 msec). For the same fat T_1, the shorter the effective repetition time TR_{eff}, the lower the magnitude of the steady state magnetization M_{ss}, as shown in Fig. 2B.

The time of the null point, $TI_{CSS\text{-}IR}$, for the steady state condition can then be calculated from Eqs. (1) and (8):

$$TI_{CSS\text{-}IR} = T_1 \ln 2 - T_1 \ln(1 + e^{-TR_{eff}/T_1}) \; . \tag{9}$$

In contrast to the STIR experiment, where the inversion time for fat suppression is dependent only on the T_1 of fat, Eq. (9) shows that the inversion time for the CSS-IR sequence is a function of T_1, repetition time, and number of slices. This dependency is illustrated in Fig. 3, where the inversion time is plotted against the number of slices for a range of repetition times. Comparing Eqs. (2) and (9), it can be shown that $TI_{CSS\text{-}IR}$ is generally shorter than TI_{STIR}, which makes the CSS-IR sequence more time-efficient than STIR. The result is that for the same repetition time, more slices can be selected using the hybrid sequence, as shown in Fig. 4.

Figure 5 shows the calculated inversion time as a function of the T_1 of fat for both STIR and CSS-IR sequences, using Eqs. (2) and (9) respectively, for a range of common values of TR_{eff}. Differentiation of Eqs. (2) and (9) shows that the rate of change of the inversion time as a function of fat T_1 for STIR is always greater than the rate of change of the inversion time for CSS-IR. The hybrid sequence thus requires a smaller range of inversion times than STIR to null signal from fat exhibiting a particular range of T_1 values, so the suppression is less dependent on the range of fat T_1 values present or the accuracy of the measured/estimated T_1 of fat.

An additional advantage of the hybrid sequence is that it can tolerate greater mis-settings of the tip angle of the chemical shift selective pulse than FATSAT. Figure 6 shows the magnitude of longitudinal fat magnetization at the time when the 90° slice selective pulse is applied, derived from Eq. (6) as a function of the effective tip angle of the previous chemical shift selective pulse, for both FATSAT and CSS-IR. For this particular example the range of tip angles that result in a residual fat magnetization of less than 5% are indicated by the arrows on the graph. For CSS-IR, this range is a 42% of the nominal 180° value for the fat selective pulse, where as for FATSAT this range is only 12% of the nominal 90° value.

All the above arguments assume a steady state condition, so we need to determine how many repetitions of the CSS-IR sequence are required to reach this steady state for the fat magnetization. If we define that the steady state condition is reached when the difference between the fat magnetization M_n and the magnetization M_{ss} is less than or equal to a predetermined value α% of M_{ss}, then:

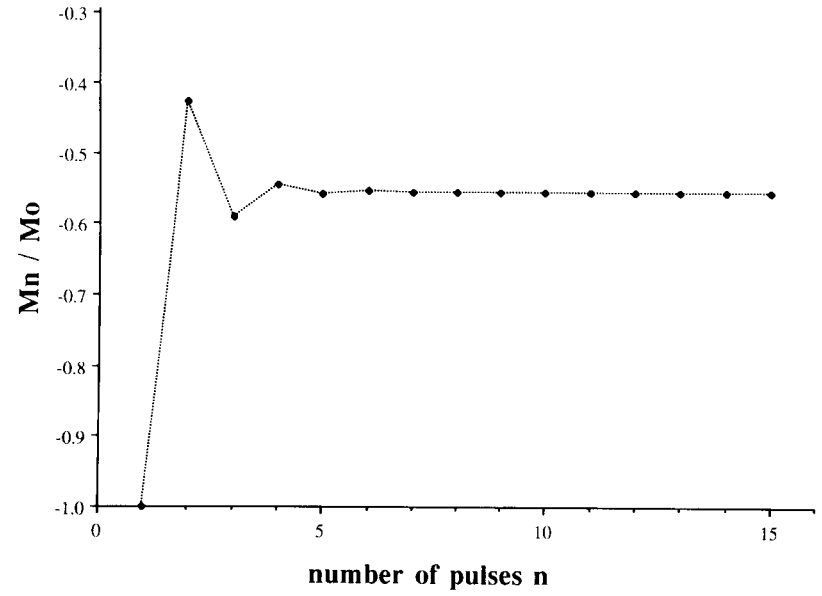

(A)

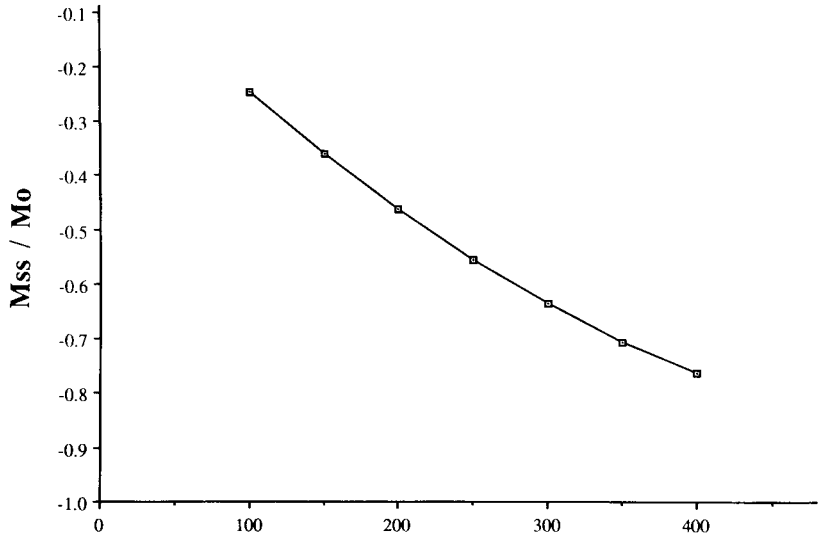

(B)

Fig. 2. (A) M_n, as a fraction of the thermal equilibrium magnetization M_o, just after each inverting pulse. The T_1 of fat is assumed to be 200 msec and the pulse repetition time is 250 msec. (B) The value of the steady state magnetization M_{ss} for the same T_1 as a function of the effective repetition time TR_{eff}.

$$\frac{|M_n - M_{ss}|}{M_{ss}} \leq \frac{\alpha}{100} \qquad (10)$$

$$n_{ss} \geq -\frac{T_1}{TR_{eff}} \ln\left[\frac{1}{2}\,\frac{\alpha}{100}\,(1 - e^{-TR_{eff}/T_1})\right] . \qquad (7)$$

or, substituting M_n and M_{ss} from Eqs. (7) and (8) respectively, the minimum number of sequence repetitions for the fat magnetization to be within α% of the steady state value M_{ss} is:

For conventional imaging conditions, n_{ss} is usually very small compared to the total number of sequence repetitions (phase encoding and signal averaging), therefore steady state for fat magnetization can be achieved

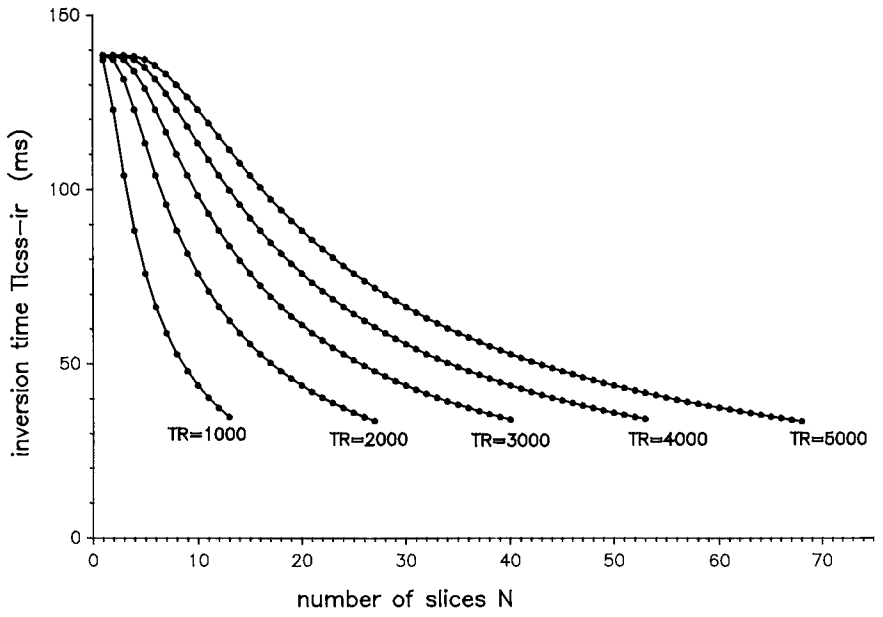

Fig. 3. The inversion time, TI_{CSS-IR}, as a function of the number of slices, N, for a range of sequence repetition times, TR. It is assumed that the fat magnetization has a T_1 of 200 msec and the total imaging time of the spin echo part of the sequence is 40 msec. The curves terminate where $N(TI_{CSS-IR} + TE) = TR$, that is, when no more slices can be fitted within the repetition time. Note that the plot is meaningful at discrete points only, the solid lines drawn for clarity.

within the first few encoding steps. Alternatively, n_{ss} can be accommodated as dummy scans at the beginning of the experiment with negligible increase of the total imaging time.

To give an example of the timing for the CSS-IR sequence; in a clinical case from the literature[12] a STIR sequence with TR = 1560 msec and TI_{STIR} = 150 msec was used to suppress signal from the orbital fat (mean T_1 of 215 msec) in a 6-slice image set of the optic nerve (white matter mean T_1 of 385 msec) in a 0.5 T clinical system. For the same data set with the same repetition time, the hybrid fat-suppression sequence would require an inversion time of TI_{CSS-IR} = 94 msec (as opposed to 150 msec), while nine dummy scans would be enough for the fat magnetization to reach a value with less than 0.01% difference from its steady state value.

METHODS

The hybrid CSS-IR sequence was evaluated, using phantoms, for its ability to suppress fat without degrading the S/N ratio for the remaining water signal. The performance of the sequence was studied for its dependence on the estimated T_1 of fat, as well as its dependence on the homogeneity of the static magnetic field, $\mathbf{B}_0$, and radiofrequency field, $\mathbf{B}_1$. Finally, the new hybrid fat suppression technique was demonstrated in vivo by imaging the abdominal region of a normal live, adult rat. All experiments involved direct comparison with a range of other common fat-suppression MRI methods. The study was performed on a SISCO-200 NMR imaging spectrometer (Spectroscopy Imaging Systems Corporation, Fremont, California) operating at 200 MHz, with a 4.7 T, 33 cm bore superconducting magnet (Oxford Instruments Limited, Oxford, UK). An imaging coil with an inner diameter of 9 cm was used for all phantom and in vivo experiments.

Fat Suppression

The aim of this part of the study was to demonstrate the ability of the CSS-IR sequence to suppress fat in the images of a water/oil phantom, in direct comparison to the conventional MRI fat-suppression techniques already mentioned (i.e., STIR and FATSAT), as well as to a single-slice chemical shift imaging (CSI) method[13]. The phantom used consisted of a glass tube (~1 cm outer diameter, ~3.5 cm height) inside a glass beaker (~2.5 cm outer diameter, ~3.5 cm height). The inner tube contained heavy white mineral oil (Aldrich Chemical Co. Ltd., Gillingham SP8 4JL, England). The beaker contained distilled water doped with ~0.6 g/l copper sulphate ($CuSO_4$) to give a solution with a T_1 of ~330 msec. The mineral oil had a mean T_1 of 200 msec. The T_1 value of each component was measured by the standard spectroscopic version of the inversion recovery technique.[14] A pilot spectrum from the phantom,

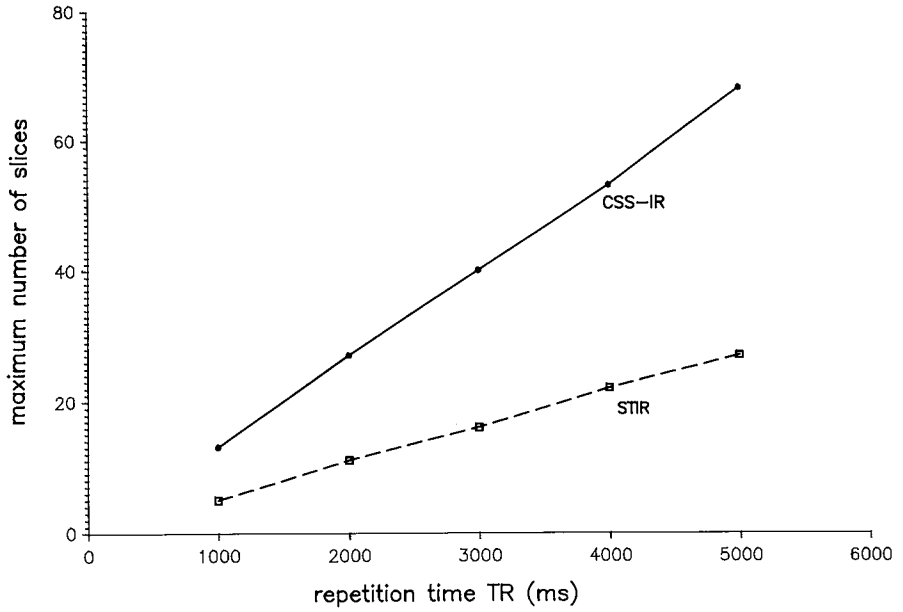

Fig. 4. The maximum number of slices which can be selected within a repetition time TR for the STIR and CSS-IR sequences. It is assumed that the fat magnetization has a T_1 of 200 msec and the total imaging time of the spin echo part of both sequences is 40 msec.

acquired prior to the imaging experiments, showed that the oil resonance frequencies occurred within a ~2 ppm (i.e., 400 Hz) range, centred ~3.6 ppm (i.e., 720 Hz) upfield from the water peak (shimmed to 0.5 ppm full width at half maximum height).

For the imaging experiment, the phantom was placed vertically and 10 cross-sectional slices of 2 mm thickness were acquired through the middle of the object. A series of imaging sequences with a fixed echo time (TE = 30 msec) was performed:

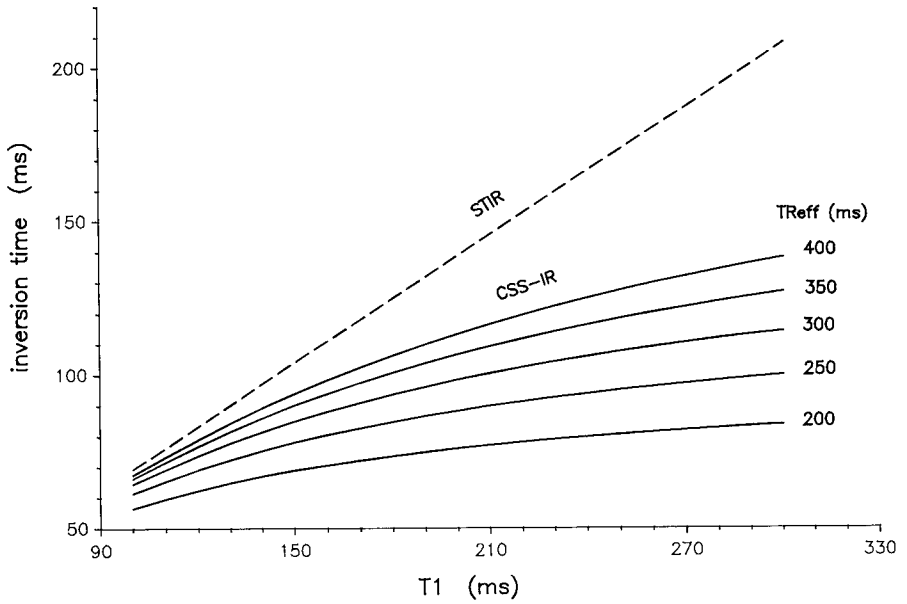

Fig. 5. The calculated inversion time as a function of fat T_1 for STIR (dashed line) and CSS-IR (solid lines), for a typical range of effective repetition times, TR_{eff}.

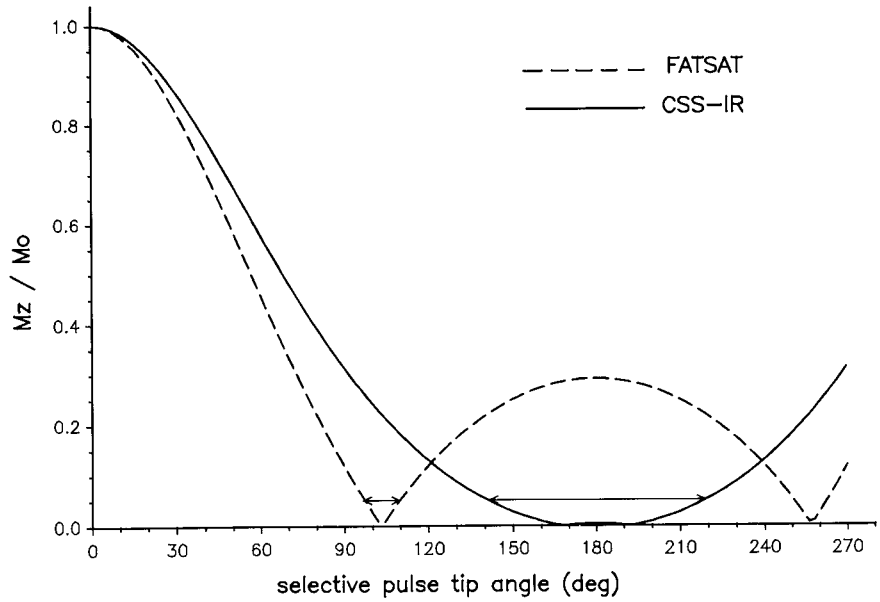

Fig. 6. The amplitude of longitudinal fat magnetization M_z (as a fraction of its thermal equilibrium value M_o) just before the application of the 90° slice selective pulse, plotted against the tip angle of the fat selective pulse for FATSAT (dashed line) and CSS-IR (solid line). The arrows indicate the range of tip angles for which fat magnetization is less than 5%. A fat T_1 of 200 msec, a TR_{eff} of 200 msec, and a duration of 25 msec for the spoiling gradient in FATSAT are assumed.

1. standard spin echo (SE) sequence (TR = 2000 msec),
2. single-slice chemical shift (CSI) imaging sequence, whereby the desired component (i.e., water) was selectively excited in the absence of all magnetic field gradients by a chemical shift selective 90° pulse prior to a 180° slice selective refocusing pulse (TR = 2000 msec),
3. conventional short inversion time inversion recovery (STIR), with TI_{STIR} = 139 msec (TR = 2640 msec),
4. selective presaturation (FATSAT) sequence, saturating the fat before each slice selective excitation of the sequence (TR = 2000 msec and spoiling gradient of 25 msec duration),
5. the new fat-suppression (CSS-IR) sequence, with TR = 2000 msec and $TI_{CSS\text{-}IR}$ = 75 msec as calculated using Eq. (9), with 12 dummy scans at the beginning of the experiment to allow for the fat magnetization to reach less than 0.01% difference from its steady state value, Eq. (11).

A diagrammatic representation of the pulse sequences is given in Fig. 7, where the shaded box represents the conventional spin-warp part of the imaging experiment, common to all sequences used. All imaging experiments were performed with a 4 × 4 cm field of view, 256 × 128 data matrix and four signal averages per phase encode step. Slice selection was performed with 5000 μsec five-lobe sinc pulses in the presence of 11.7 mT/m linear magnetic field gradient, giving a slice thickness of 2 mm, while the chemical shift selection used 2500 μsec Gaussian pulses of 800 Hz frequency bandwidth, that is, 4 ppm at 4.7 T.

The oil signal was calculated for all images by measuring the mean signal intensity from a 25 mm^2 (i.e., 512 pixels) region of interest, while the noise was determined by measuring the mean intensity from a 200 mm^2 (i.e., 4096 pixels) region of interest in the background. The standard error of the mean signal intensity (SEM) was calculated using a standard procedure from the literature.[15] It should be noted that all images were magnitude images, therefore we would expect a positive bias to the measurements of any low-level signal, such as the suppressed oil signal.[16,17] However, no effort was made to correct this positive bias, as our main concern in this study was a relative evaluation of the efficiency of different methods to suppress the oil signal, and not the deduction of absolute values.

T_1 Dependency

Fat suppression in both STIR and CSS-IR sequences depends on the accuracy of the determination of the fat T_1, as discussed in the theory (Fig. 5). A series of experiments was performed to study the dependency of fat-suppression on the accuracy of the estimated fat T_1 value, that is the sensitivity of fat-suppression to the inversion time used.

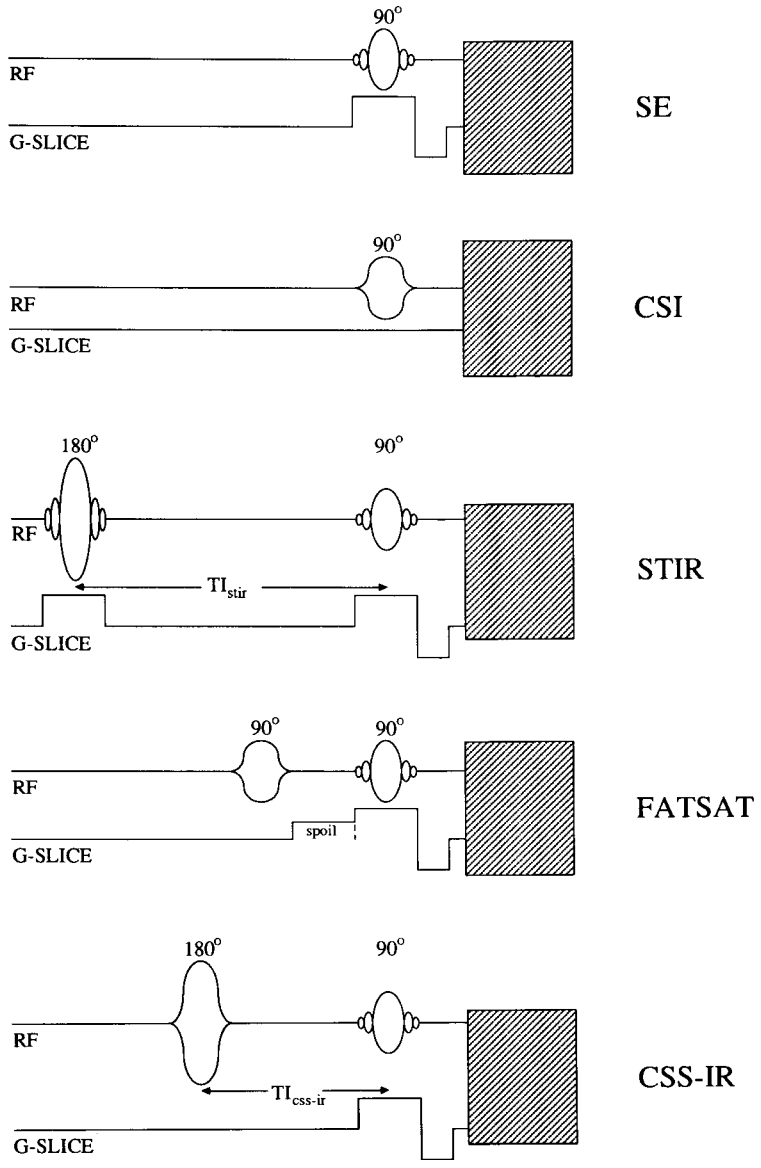

Fig. 7. Pulse sequence diagrams for all techniques used. SE: conventional spin echo; CSI: single-slice chemical shift imaging sequence; STIR; FATSAT; CSS-IR. The shaded box, common to all sequences, represents the conventional spin-warp method.

The hybrid CSS-IR and the conventional STIR sequence were performed as above. The experiments were then repeated for a range of different inversion times, $TI_{CSS\text{-}IR}$ and TI_{STIR}. These TI values were calculated using Eqs. (9) and (2) respectively, assuming hypothetical T_1 values for the oil ranging up to ±60% of the actual T_1 value of 200 msec (hypothetical T_1 values were in the range from 80 to 300 msec). The oil signal in all experiments was measured as before.

B_1 Dependency

The aim of this part of the study was to investigate the dependency of fat suppression on the effective tip angle of the fat selective pulse, as discussed in the theory (Fig. 6). The hybrid CSS-IR and the conventional FATSAT sequence were performed as in the first part of the study. The experiments were then repeated for a range of different effective tip angles for the chemical shift selective pulses, that is, the 90° saturation pulse in the FATSAT sequence, and the 180° inversion pulse in the new sequence, respectively. The tip angles were calculated to be within a range from −44% to +41% of the nominal value for the fat selective pulse in both sequences, that is, from 50° to 127° for the presaturating pulse in FATSAT, and from 101° to 254° for the inverting pulse in CSS-IR. Note that although

variations in $\mathbf{B}_1$ are generally relatively small for conventional imaging coils in clinical systems, the radiofrequency field can be greatly degraded in surface coil imaging.

B_0-Homogeneity Dependency

As both FATSAT and CSS-IR sequences employ chemical shift selective pulses, the fat suppression depends on the spectral resolution of the two resonances. Sufficient fat suppression can always be ensured by the use of a rather broad frequency selective pulse to excite or invert, respectively, the whole range of fat resonances. However, in situations where the spectral resolution is degraded, for example by regional $\mathbf{B}_0$ inhomogeneities, such a pulse may also suppress part of the water signal. This experiment was, therefore, intended to study the effects of FATSAT and the hybrid fat-suppression technique on the water signal in such cases.

The hybrid CSS-IR and the conventional FATSAT sequence were performed as in the first part of the study. The experiments were then repeated for a range of different effective bandwidths of the chemical shift selective pulses (centered on the oil resonance). The bandwidths were calculated to cover the whole possible range of frequency selection, from suppressing just the oil peak (2 ppm), to suppressing the whole spectrum (10 ppm).

In Vivo Studies

A normal 350 g adult male Wistar rat was placed in the magnet in a prone position, under anaesthesia induced and maintained by 1% (v/v) halothane in oxygen flowing at a rate of 1 l/min. A series of inversion recovery spectra were obtained with a range of inversion times from which the T_1 of bulk fat was estimated to be ~326 msec. Fifteen axial slices, 2.4 mm thick, in the abdominal region were then acquired using a spin-echo sequence with TR = 3000 msec, STIR with TR = 5115 msec and TI_{STIR} = 226 msec, FATSAT with TR = 3000 msec and the CSS-IR sequence with TR = 3000 msec and $TI_{CSS\text{-}IR}$ = 85 msec. All imaging experiments were performed with TE = 30 msec, 8 × 8 cm field of view, 256 × 256 data matrix and four signal averages per phase-encode step.

RESULTS AND DISCUSSION

Fat Suppression

The fifth slice from each 10-slice data set is shown in Fig. 8. The chemical shift artifact is well illustrated in the spin-echo image (Fig. 8A), where the fat signal is displaced relative to water in the frequency-encode (horizontal) direction. A bright/dark ring appears at the interface of the two components because of the superposition of the misregistered signals. Fig. 8B is the water-only image of the same slice, obtained with the CSI sequence. In the STIR image (Fig. 8C), the degradation of the image quality is apparent as signal from the water compartment is significantly suppressed. Images acquired using fat saturation (Fig. 8D) and the CSS-IR sequence (Fig. 8E), on the other hand, exhibit both good fat suppression and image quality.

Table 1. Fat and water signal, as well as noise mean intensities (arbitrary units) corresponding to the images in Fig. 8

	Oil signal	Water signal
Spin echo	110.3 ± 0.41	306.8 ± 0.41
CSI	12.2 ± 0.29	297.5 ± 0.40
STIR	12.1 ± 0.28	51.1 ± 0.39
FATSAT	12.5 ± 0.30	298.7 ± 0.40
CSS-IR	12.5 ± 0.29	307.8 ± 0.41
Noise	11.5 ± 0.10	11.5 ± 0.10

The mean intensities as well as the standard error of the mean (SEM) have been calculated as described in the text.

The oil and water signals for all sequences are given in Table 1. If we define a 100% suppression to be the suppression of the high signal in the spin-echo experiment down to the noise level, the three conventional fat-suppression techniques and the new hybrid sequence result in about 99% suppression for the oil signal. The residual oil signal in CSI and FATSAT images may be attributed to the protons of the −OH group, which appears in a low concentration in the oil, and have the same chemical shift range as the −OH protons of the water molecule. A further increase in the residual signal in the FATSAT image may occur due to the partial recovery of the fat signal in the time between the chemical shift selective pulse and the following spin echo part of the experiment. In the STIR image, the residual signal may be due to the presence of a range of T_1/s in the oil, which correspond to a range of null-point values. It might be expected that in CSS-IR both factors would combine to give an even greater residual oil signal. However, as is shown by the following experiments, fat-suppression by the CSS-IR sequence is significantly less dependent on the oil T_1 than it is in the STIR experiment. As all four sequences give such good fat suppression, no further experiments were performed to study the origin of any residual oil signal.

T_1 Dependency

Figure 9 shows the residual oil signal in the STIR and CSS-IR sequence images as a function of the "assumed" value of oil T_1 used to calculate the inversion time for both sequences. In the STIR images, suppression of the oil signal greater than 95% is achieved only over a lim-

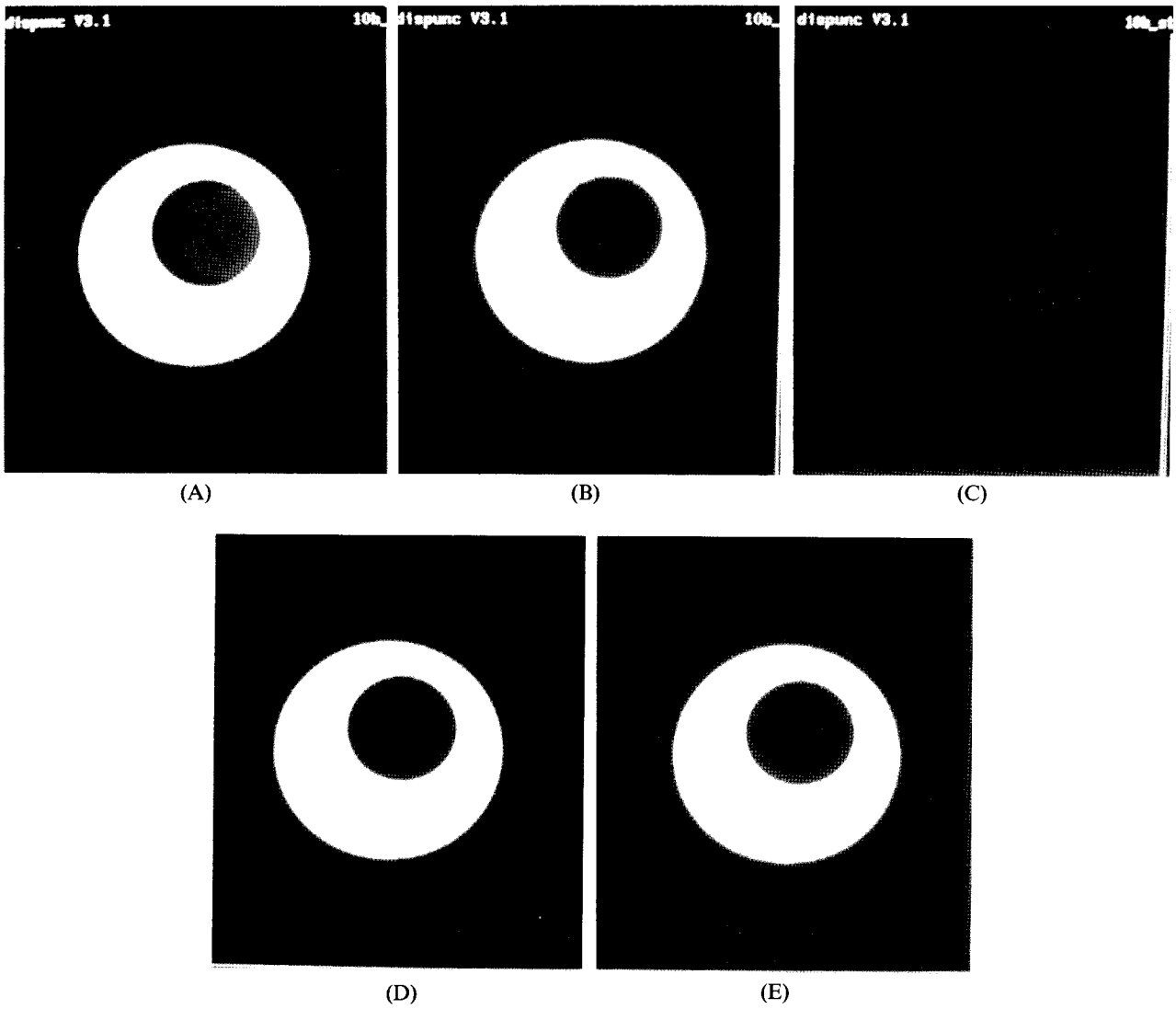

Fig. 8. Phantom images from the 5th slice of each 10-slice data set acquired using: (A) a spin echo sequence; (B) CSI; (C) STIR; (D) FATSAT; and (E) CSS-IR. The phantom consists of a tube containing oil, placed within a beaker full of water.

ited T_1 range of 80 msec around the actual oil T_1 value of 200 msec, and drops down to 74% or 78%, respectively, for "assumed" T_1 values 60% shorter or longer than the actual oil T_1. In contrast, the CSS-IR sequence gives a fat-suppression greater than 95% over the whole range of the "assumed" T_1 values used in this series of experiments (i.e., 220 msec). These results show that fat suppression by the proposed hybrid sequence is relatively independent of the value of fat T_1, as predicted by the theoretical analysis (see Fig. 5).

B_1 Dependency

Figure 10 shows the residual oil signal in the FATSAT and CSS-IR sequence images as a function of the effective tip angle for the selective pulse. For the FATSAT sequence fat suppression is greater than 95% only for the limited range of effective tip angles from 80° to 101°, which corresponds to a mis-setting of −11% to 12% of the nominal 90° value. For the extreme value of 50° used in this experiment (−44% mis-setting), the fat suppression drops as low as 54%. The CSS-IR sequence, on the other hand, shows the same efficient performance of more than 95% fat suppression for the much wider range of effective tip angles from 113° to 213°. This corresponds to a mis-setting of −37% to 18% of the desired 180° value. Even for the extreme values of 101° or 254° (−44% and 41% mis-setting), the fat suppression is as high as 91% and 81% respec-

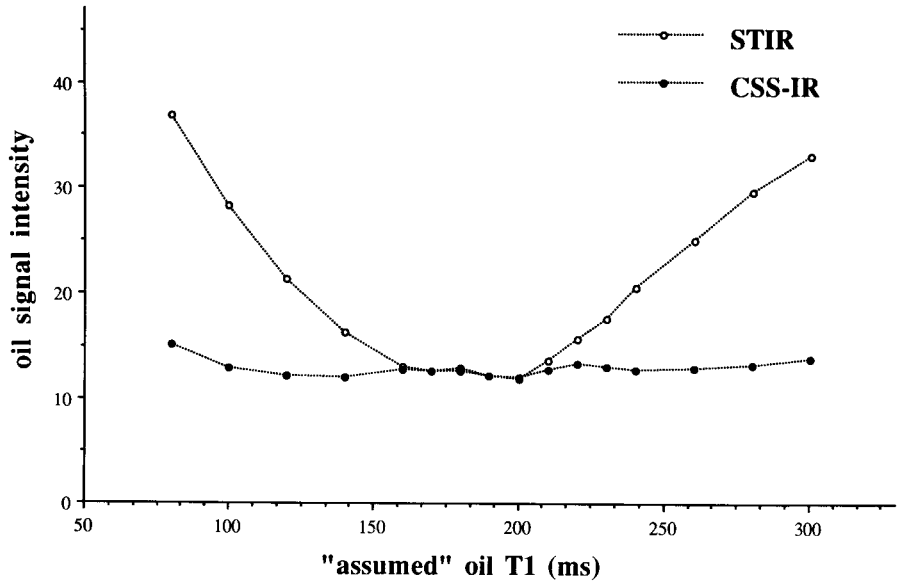

Fig. 9. The measured oil signal intensity (arbitrary units) plotted against the "assumed" value of oil T_1 (used to calculate the inversion time) for both STIR (o) and the CSS-IR sequence (●).

tively. These results show that fat suppression by the proposed hybrid sequence is high for a significantly wider range of tip angles for the fat selective pulse, as predicted by the theoretical analysis (see Fig. 6).

B_0-Homogeneity Dependency

Figure 11 shows the water signal in the images from both the FATSAT and the CSS-IR sequences as a function of the effective frequency bandwidths for the chemical shift selective pulses. All experiments showed fat suppression equal to or better than 99%, so the oil signal has not been plotted. Selective pulses centred on the oil resonance with bandwidths up to 6 ppm should not affect the water protons whose resonances lie within a 0.5 ppm range centered 3.6 ppm away. This agrees with the experimental results for both sequences, as pre-

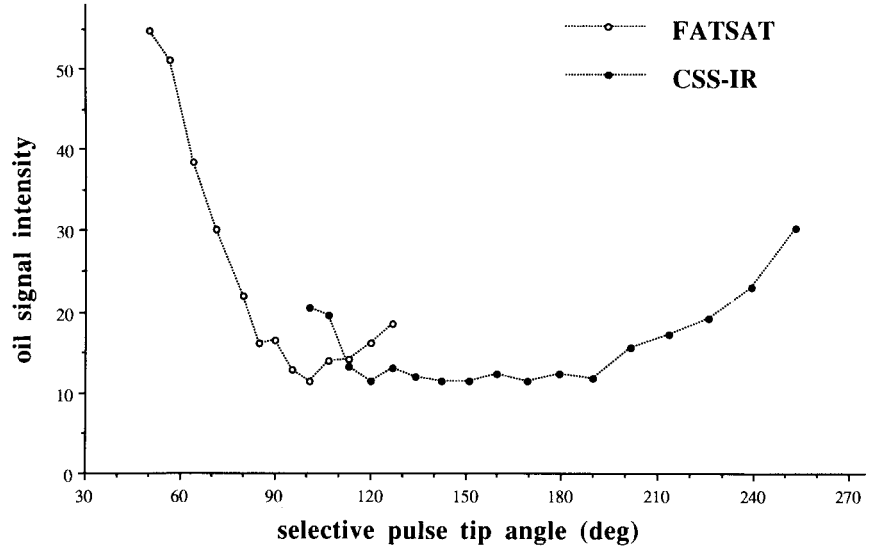

Fig. 10. The measured oil signal intensity (arbitrary units) plotted against the effective tip angle of the chemical shift selective pulse, for FATSAT (o) and the CSS-IR sequence (●).

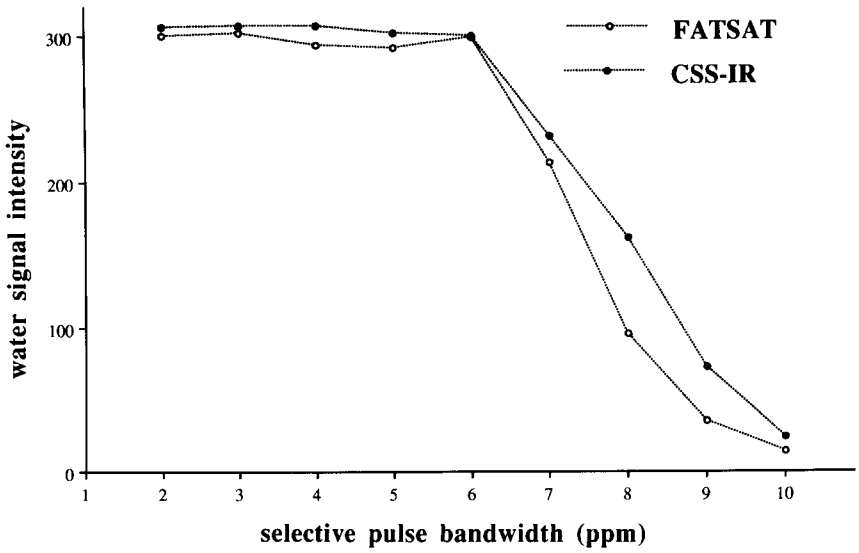

Fig. 11. The water signal intensity (arbitrary units) plotted against the bandwidth of the chemical shift selective pulses (centered on the oil resonance), for FATSAT (o) and the hybrid CSS-IR sequence (●).

sented in Fig. 11. Pulses with frequency bandwidths wider than 6 ppm are expected to affect both the oil and water resonances, and this can be seen in Fig. 11, where the water signal is progressively suppressed as the pulse becomes less selective. However, the remaining water signal in the images acquired with the hybrid sequence is always significantly larger than in the corresponding FATSAT images. Although in the FATSAT sequence, all the "selected" magnetization excited by the primary 90° pulse is completely saturated, in the CSS-IR sequence the magnetization affected by the chemical shift selective pulse is merely inverted and is nulled only if the inversion time corresponds to its null point. Since water generally has a much longer T_1 relaxation time than fat, then even if it is all inverted by the selective pulse of the CSS-IR sequence it will still yield some residual signal, its value being dependent on the water T_1 and the sequence parameters (Eq. (9)).

In Vivo Studies

Figures 12 and 13 show the images of two transverse slices across the abdominal region of a normal rat as obtained by spin-echo, STIR, FATSAT, and CSS-IR sequences. In Fig. 12, note the abdominal fat which surrounds the kidneys. In the short TE spin echo image (Fig. 12A), the high signal intensity from the fat reduces the dynamic range available for the water signal and the fine anatomical detail within the kidneys is lost. In the STIR image (Fig. 12B) fat signal is suppressed but only the central region of the kidneys (calyces and renal pelvis) can be clearly seen, because of the overall degradation of S/N and the high T_1 contrast. The kidneys are well illustrated in the other two fat-suppressed images (Figs. 12C and 12D). Figure 13 shows a cross section at the level of the bladder. In the spin echo image (Fig. 13A) the chemical shift artifact is again apparent, with the signal of the abdominal fat being superimposed on the water signal, creating a bright ring at the left side of the bladder wall. Fat suppression in the following images (Figs. 13B, 13C, and 13D) has removed the artifact and the bladder is clearly outlined. Once again, in the STIR image (Fig. 13B) the low S/N ratio for the tissues surrounding the bladder results in a significant loss of the overall anatomical detail. Note that although the CSS-IR sequence (Fig. 13D) gives efficient fat suppression, the FATSAT image (Fig. 13C) still suffers from some chemical shift artifact, probably due to regional differences in $\mathbf{B}_1$ homogeneity.

CONCLUSIONS

We have investigated a hybrid pulse sequence for fat suppression in proton magnetic resonance imaging and have demonstrated, both theoretically and experimentally, the efficiency of the method compared to its most closely related conventional fat-suppression techniques, namely STIR and FATSAT. The new sequence has been proven to give the same efficient fat suppression as the other conventional methods employed, in both phantom and in vivo studies. In addition, the technique has shown better performance than STIR or FATSAT in several situations where parameters, such as inversion

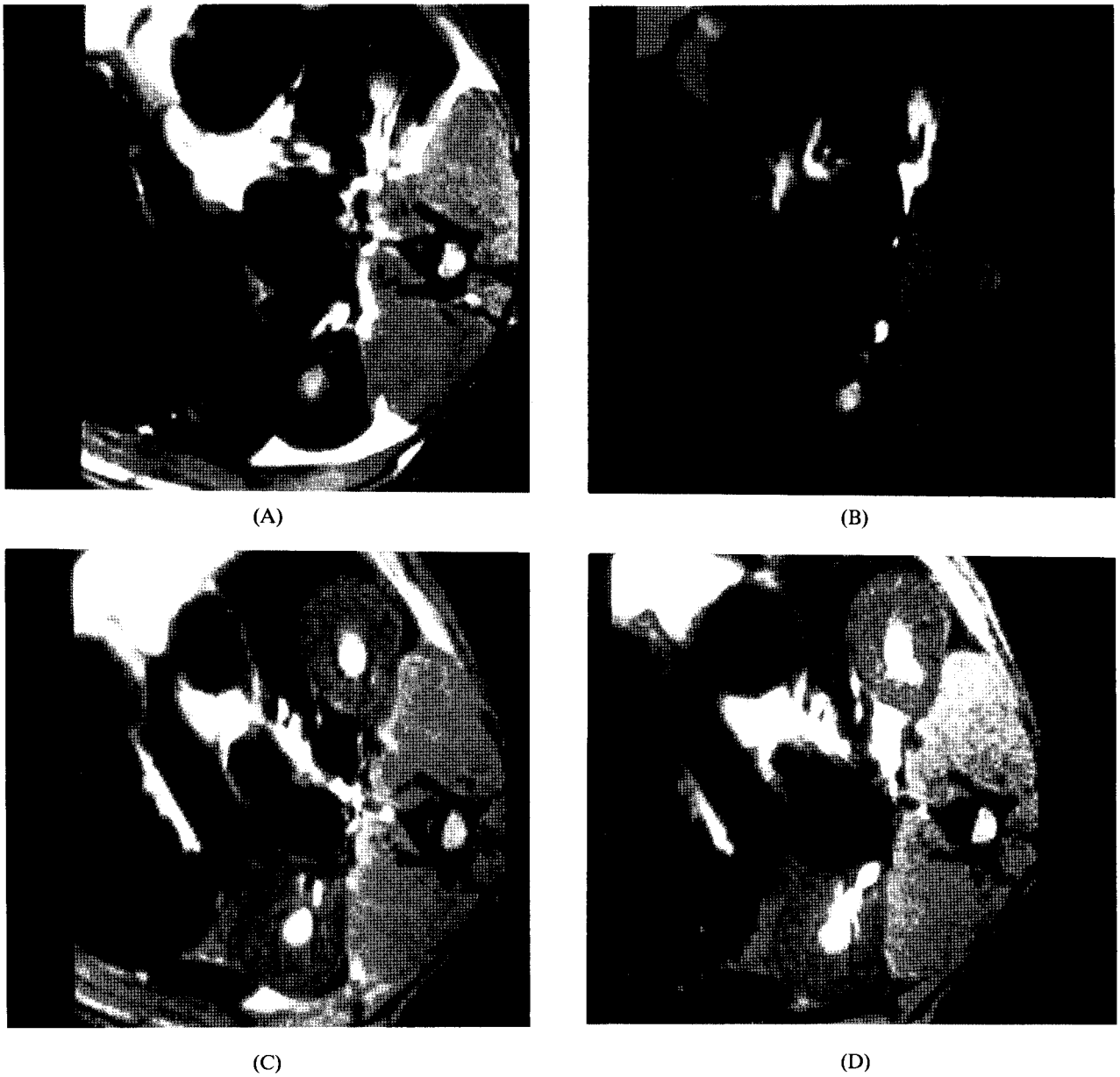

Fig. 12. Transverse image of the abdominal region of a live normal rat at the level of the kidneys, produced using: (A) a spin-echo sequence; (B) STIR; (C) FATSAT; and (D) CSS-IR.

time as well as tip angle and frequency bandwidth of the fat selective pulse, were mis-set.

The hybrid CSS-IR sequence combines a fat selective pulse with the inversion recovery approach of STIR. However, the inversion time is generally significantly shorter than that used in the conventional STIR sequence, thus allowing shorter repetition times or, alternatively, more slices to be selected within the same imaging time. While in the STIR sequence fat suppression is strongly dependent upon the fat T_1 value used to calculate the inversion time, both theory and experiments show that in the hybrid sequence the null-point for the fat spins is, in general, effectively independent of T_1 for a significant range of fat T_1 values. This ensures efficient fat suppression even in the cases where either the fat T_1 is not accurately known prior to imaging or there is a wide range of fat T_1 values.

The CSS-IR sequence has been shown to provide good fat suppression for a wider range of mis-settings of the chemical shift selective pulse tip angle than the FATSAT sequence. Even though modern instrumentation affords only a few percent variation in $\mathbf{B}_1$ field

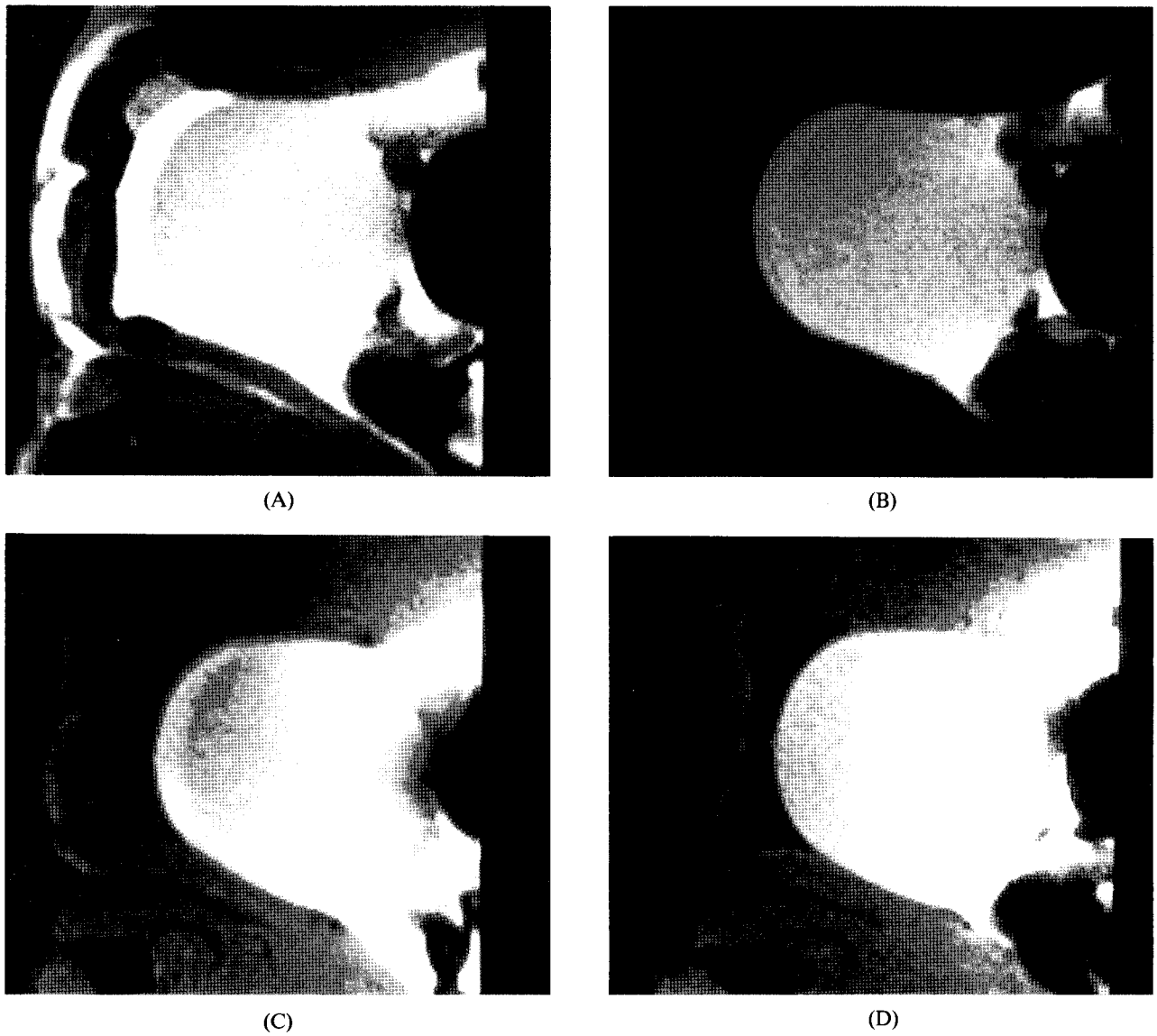

Fig. 13. Transverse image of the abdominal region of a live normal rat at the level of the bladder, produced using: (A) a spin-echo sequence; (B) STIR; (C) FATSAT; and (D) CSS-IR.

homogeneity in the central imaging volume, the field may be rapidly degraded near the edges of the coil. This becomes particularly important in the suppression of subcutaneous fat which is nearest to this inhomogeneous region. One can also envisage future application of CSS-IR to fat-suppressed imaging using surface or internal coils.

The sensitivity of the FATSAT sequence to the tip angle of the chemical shift selective pulse seems to be one of its most important limitations. The performance of this conventional technique could be improved by applying the initial 90° chemical shift selective pulse and the following spoil gradient more than once. In fact, this scheme has been used in clinical practice with three repetitions of the 90°-spoil saturation scheme prior to the following read-out part of the sequence. Note that the three successive gradient pulses should ideally be applied in different axes, in order to avoid the formation of unwanted stimulated echoes. Although this version of FATSAT may be less dependent on $\mathbf{B}_1$ than the conventional sequence, one should also note that there is an increase in RF power deposition, as well as an increase in the overall imaging time. Other, less closely related fat-suppression techniques have also been reported to be less $\mathbf{B}_1$ dependent than FATSAT. Such an example is the selective echo chemical shift im-

aging (SECSI) sequence.[18] In this spin-echo method the 180° pulse is chemical shift selective and refocuses only, say, the water protons within the slice selected by a prior 90° excitation pulse. This method, as well as its combination with the FATSAT experiment, was shown to be far less dependent on $\mathbf{B}_1$ and $\mathbf{B}_0$ variations than the conventional FATSAT sequence.[19] However, one should note that while the chemical shift 180° pulse refocuses water spins within the selected slice, it will also invert water magnetization in the rest of the imaging volume. Immediate repetition of such a sequence to acquire a different slice, could result in a highly T_1-weighted water image. Therefore, if multi-slice imaging is desired, one would expect a similar S/N degradation as in the STIR image.

Fat suppression using a chemical shift selective pulse requires a relatively high and homogeneous static magnetic field in order to resolve the fat and water resonances. Thus fat suppression sequences that are based merely on this principle may give less acceptable results in cases where the static field is regionally degraded by susceptibility differences within the imaging object, for instance when imaging the optical nerve and musculoskeletal system. Even though the CSS-IR method uses chemical shift selection of fat resonances, we have shown that a wider selective pulse will always ensure good fat suppression without reducing the water signal as much as in the FATSAT sequence.

Acknowledgments—We wish to acknowledge many useful discussions with Drs. Steve R. Williams and Mark A. Horsfield. We would like to thank U.L.I.R.S. for use of their imaging facility. Display software (*dispim*) was kindly supplied by Dr. Dave Plummer. This work was financially supported by State Scholarship Foundation, Greece and The British Council (E.K), and the Multiple Sclerosis Society of Great Britain and Northern Ireland (G.J.B and P.S.T).

REFERENCES

1. Kaldoudi, E.; Williams, S.C.R. Fat and water differentiation by nuclear magnetic resonance imaging. *Concepts Magn. Reson.* 4:53–71; 1992.
2. Hawkins, C.P.; Williams, S.C.R.; Barker, G.J.; Youl, B.; Revesz, T.; Newcombe, J.; Brar, A.; MacManus, D.G.; du Boulay, E.P.G.H.; McDonald, W.I. Lipid imaging to detect myelin breakdown in multiple sclerosis. *Neuroradiol.* 33(suppl.):404–405; 1991.
3. Altbach, M.I.; Mattingly, M.A.; Brown, M.F.; Gmitro, A.F. Magnetic resonance imaging of lipid deposits in human atheroma via a stimulated-echo diffusion-weighted technique. *Magn. Reson. Med.* 20:319–326; 1991.
4. Bydder, G.M.; Young, I.R. MR imaging: Clinical use of the inversion recovery sequence. *J. Comput. Assist. Tomogr.* 9:659–675; 1985.
5. Golfieri, R.; Baddeley, H.; Pringle, J.S.; Souhami, R. The role of the STIR sequence in magnetic resonance imaging examination of bone tumours. *Br. J. Radiol.* 63: 251–256; 1990.
6. Shuman, W.P.; Baron, R.L.; Peters, M.J.; Tazioli, P.K. Comparison of STIR and spin echo MR imaging at 1.5 T in 90 lesions of the chest, liver and pelvis. *Am. J. Roentgenol.* 152:853–859; 1989.
7. Rosen, B.R.; Wedeen, V.J.; Brady, T.J. Selective saturation NMR imaging. *J. Comput. Assist. Tomogr.* 8: 813–818; 1984.
8. Haase, A.; Frahm, J.; Hanicke, W.; Matthaei, D. H-1 NMR chemical shift selective (CHESS) imaging. *Phys. Med. Biol.* 30:341–344; 1985.
9. Keller, P.J.; Hunter, W.W.; Schmalbrock, P. Multisection fat-water imaging with chemical shift selective presaturation. *Radiology* 164:539–541; 1987.
10. Oh, C.H.; Hilal, S.K.; Cho, Z.H. Selective partial inversion recovery (SPIR) in steady state for selective saturation magnetic resonance imaging (MRI). In: Book of Abstracts: Seventh Annual Meeting of the Society of Magnetic Resonance in Medicine (Vol 2). San Francisco: SMRM; 1988: 1042.
11. Merchant, T.E.; Thelissen, G.R.P.; Kievit, H.C.E., Oosterwaal, L.J.M.P.; Bakker, C.J.G.; de Graaf, P.W. Breast disease evaluation with fat-suppressed magnetic resonance imaging. *Magn. Reson. Imaging* 10:335–340; 1992.
12. Johnson, G.; Miller, D.H.; MacManus, D.; Tofts, P.S.; Barnes, D.; du Boulay, E.P.G.H.; McDonald, W.I. STIR sequences in NMR imaging of the optic nerve. *Neuroradiol.* 29:238–245; 1987.
13. Hall, L.D.; Sukumar, S.; Talagala, S.L. Chemical-shift-resolved tomography using frequency-selective excitation and suppression of specific resonances. *J. Magn. Reson.* 56:275–278; 1984.
14. Hahn, E.L. An accurate nuclear magnetic resonance method for measuring spin-lattice relaxation times. *Phys. Rev.* 76:145–146; 1949.
15. Edelstein, W.A.; Bottomley, P.A.; Pfeifer, L.M. A signal-to-noise calibration procedure for NMR imaging systems. *Med. Phys.* 11:180–185; 1984.
16. Henkelman, R.M. Measurement of signal intensities in the presence of noise in MR images. *Med. Phys.* 12:232–233; 1985.
17. Tofts, P.S.; Johnson, G. Correction for Rayleigh noise in an NMR magnitude image when measuring T_2 at low values of signal-to-noise ratio. In: Book of Abstracts: Fifth Annual Meeting of the Society of Magnetic Resonance in Medicine. Montreal: SMRM; 1986: 1450–1451.
18. Joseph, P.M. A spin echo chemical shift imaging technique. *J. Comp. Assist. Tomogr.* 9:651–658; 1985.
19. Joseph, P.M.; Shetty, A. A comparison of selective saturation and selective echo chemical shift imaging techniques. *Magn. Reson. Imaging* 6:421–430; 1988.